J|A|C|S
ARTICLES
Published on Web 11/13/2002

Investigation of the [Sm{N(SiMe$_3$)$_2$}$_2$] Reducing System in THF. Rate and Mechanistic Studies[1]

Edamana Prasad, Brian W. Knettle, and Robert A. Flowers, II*

Contribution from the Department of Chemistry and Biochemistry, Texas Tech University, Box 41061, Lubbock, Texas 79409-1061

Received August 12, 2002

Abstract: The reductant [Sm{N(SiMe$_3$)$_2$}$_2$] was examined by cyclic voltammetry and UV−vis spectroscopy. Rate constants and activation parameters for the reduction of 1-iodobutane, 2-butanone, and methyl-acetoacetate by [Sm{N(SiMe$_3$)$_2$}$_2$] were measured in THF by stopped-flow absorption decay experiments. Comparison with SmI_2 and SmI_2−HMPA shows that the redox potential of [Sm{N(SiMe$_3$)$_2$}$_2$] is intermediate between the SmI_2-based reductants, yet it reduces alkyl iodides and ketones at a faster rate than the powerful combination of SmI_2 and HMPA. The activation data for reduction of alkyl iodides and ketones by [Sm{N(SiMe$_3$)$_2$}$_2$] are consistent with highly ordered transition states having low activation barriers. All of these results taken together suggest that the mechanism of reduction of alkyl iodides and ketones by [Sm{N(SiMe$_3$)$_2$}$_2$] has more inner-sphere character than reduction by SmI_2 or Sm−(HMPA) complexes. The change in the ET mechanism is attributed to the unique structure of the [Sm{N(SiMe$_3$)$_2$}$_2$] complex.

Introduction

Reagents based on samarium have widespread use in organic synthesis.[2] Most notably, SmI_2 is recognized as the most useful of these because it is easy to prepare, has moderate solubility in electron donor solvents, and is stable if stored in an inert atmosphere.[3] Unlike many reagents, SmI_2 is capable of promoting a number of distinctly different types of bond-forming processes through radical and anionic intermediates.[4] While SmI_2 is capable of reducing activated substrates such as α,β unsaturated carbonyls or alkyl iodides, more forcing conditions are required for substrates that are more difficult to reduce through single electron transfer (SET) such as alkyl bromides and chlorides or ketones.[5] In these more recalcitrant cases, promoters such as HMPA,[6] transition metal catalysts,[7] inorganic acids,[8] bases,[9] and even light[10] can be used to induce reactions of SmI_2.

The most utilized additive in reactions of SmI_2 is HMPA. Not only does HMPA increase the rate of SmI_2-mediated reactions, but it also enhances the diastereoselectivity of many reactions.[11] Coordination of HMPA to SmI_2 produces a sterically encumbered reductant.[12] Although many reactions require using SmI_2−HMPA for success, the high carcinogenicity of HMPA makes this approach less attractive. Other basic cosolvents capable of acting as ligands have been utilized in reactions of SmI_2. These include DMPU[13] and nitrogen donor solvents.[14] Although all of these have found uses in a number of reactions, none provide the general utility of HMPA.

One of the other limits of Sm(II) chemistry as presently utilized is the requirement of electron donor solvents. Most Sm(II) chemistry is carried out in THF. While this solvent is reasonable for many applications, it is a good hydrogen atom donor and can terminate certain radical reactions.[15] Reactions have been reported in other solvents such as tetrahydropyran[16] and acetonitrile, but appear to have limited utility.[17] Recently, reports on the preparation of SmI_2−HMPA in benzene have appeared, but the general efficacy of this reducing system has not been explored.[18]

We became interested in examining a Sm-based reducing system that did not have the limitations described above. We were intrigued by {Sm[N(SiMe$_3$)$_2$]$_2$(THF)$_2$} described by Evans

* To whom correspondence should be addressed. E-mail: robert.flowers@ttu.edu.

(1) This paper is dedicated to Professor John W. Larsen in deep appreciation for his mentoring, advice, and friendship.
(2) Steel, P. G. *J. Chem. Soc., Perkin Trans. 1* **2001**, 2727.
(3) Curran, D. P.; Fevig, T. L.; Jasperse, C. P.; Totleben, M. J. *Synlett* **1992**, 943.
(4) Molander, G. A.; Harris, C. R. *Chem. Rev.* **1996**, *96*, 307.
(5) Molander, G. A. *Chem. Rev.* **1992**, *92*, 29.
(6) Inanaga, J.; Ishikawa, M.; Yamaguchi, M. *Chem. Lett.* **1987**, 1485.
(7) Inanaga, J.; Yokoyama, Y.; Baba, Y.; Yamaguchi, M. *Tetrahedron Lett.* **1991**, *32*, 5559.
(8) Kamochi, Y.; Kudo, T. *Tetrahedron* **1992**, *48*, 4301.
(9) Kamochi, Y.; Kudo, T. *Tetrahedron Lett.* **1991**, *32*, 3511.
(10) Ogawa, A.; Sumino, Y.; Nanke, T.; Ohya, S.; Sonada, N.; Hirao, T. *J. Am. Chem. Soc.* **1997**, *119*, 2745.
(11) Molander, G. A.; McKie, J. A. *J. Org. Chem.* **1992**, *57*, 3132.
(12) For crystallographic studies, see: (a) Hou, Z.; Wakatsuki, Y. *J. Chem. Soc., Chem. Commun.* **1994**, 1205. (b) Hou, Z.; Zhang, Y.; Wakatsuki, Y. *Bull. Chem. Soc. Jpn.* **1997**, *70*, 149−153. For solution studies, see: (c) Shotwell, J. B.; Sealy, J. M.; Flowers, R. A., II. *J. Org. Chem.* **1999**, *64*, 5251. (d) Knettle, B. W.; Flowers, R. A., II. *Org. Lett.* **2001**, *3*, 2321. (e) Enemaerke, R. J.; Hertz, T.; Skrydstrup, T.; Daasbjerg, K. *Chem.-Eur. J.* **2000**, *6*, 3747.
(13) Haesegawa, E.; Curran, D. P. *J. Org. Chem.* **1993**, *58*, 5008.
(14) Cabri, W.; Candiani, I.; Colombo, M.; Franzoi, L.; Bedeschi, A. *Tetrahedron Lett.* **1995**, *36*, 949.
(15) Newcomb, M.; Kaplan, J. *Tetrahedron Lett.* **1988**, *29*, 3449.
(16) Namy, J.-L.; Colomb, M.; Kagan, H. B. *Tetrahedron Lett.* **1994**, *35*, 1723.
(17) Hamann, B.; Namy, J.-L.; Kagan, H. B. *Tetrahedron* **1996**, *52*, 14225.
(18) (a) Kunishima, M.; Yoshimura, K.; Nakata, D.; Hioki, K.; Tani, S. *Chem. Pharm. Bull.* **1999**, *47*, 1196. (b) Kunishima, M.; Hioki, K.; Tani, S.; Kato, A. *Tetrahedron Lett.* **1994**, *35*, 7253. (c) Kunishima, M.; Hioki, K.; Kono, K.; Sakuma, T.; Tani, S. *Chem. Pharm. Bull.* **1994**, *42*, 2190. (d) Kunishima, M.; Hioki, K.; Ohara, T.; Tani, S. *J. Chem. Soc., Chem. Commun.* **1992**, 219.

and co-workers.[19] The $\{Sm[N(SiMe_3)_2]_2(THF)_2\}$ complex (henceforth referred to as $[Sm\{N(SiMe_3)_2\}_2]$) is soluble in a range of solvents from THF to hexane. The trimethylsilyl amide ligand provides a steric component (presumed to be important in Sm−HMPA reactions) and also affords enhanced solubility. Although numerous reports have appeared that cite the original Evans paper, only a recent elegant paper by Keough uses this complex to study an organic reaction.[20] Herein we report our initial electrochemical, spectroscopic, and rate studies on this reagent. Kinetic studies of reactions with 1-iodobutane, 2-butanone, and methylacetoacetate were carried out in THF and compared to SmI_2 and $[Sm(HMPA)_6]I_2$. This work shows that while $[Sm\{N(SiMe_3)_2\}_2]$ is a very reactive reductant, it behaves in a unique manner as compared to SmI_2.

Experimental Section

Materials and General Procedures. THF was distilled from sodium benzophenone ketyl, under a nitrogen atmosphere. Dried solvents were stored in an Innovative Technology, Inc., drybox containing a nitrogen atmosphere and a platinum catalyst for drying. The SmI_2 and $[Sm\{N(SiMe_3)_2\}_2]$ were prepared according to reported procedures.[21] The concentration of the Sm complexes was determined by iodometric titration.[12c] Methylacetoacetate, 2-butanone, and 1-iodobutane were received from Aldrich and distilled under vacuum from CaO or $MgSO_4$ before use.

The redox potentials of all Sm(II) reagents in THF were independently measured by cyclic voltammetry employing a BAS 100B electrochemical analyzer. The working electrode was a standard glassy carbon electrode. The electrode was polished with polishing alumina and cleansed in an ultrasonic bath. The auxiliary electrode was a platinum wire, and the reference electrode was a saturated $Ag/AgNO_3$ electrode. The scan rate for all experiments was 100 mV/s. The electrolyte was either tetrabutylammonium hexafluorophosphate or LiI. The concentration of the Sm(II) species in each experiment was 0.5 mM. All solutions were prepared in the drybox and transferred to the electrochemical analyzer for analysis.

Determination of the UV−vis spectra for SmI_2 and $[Sm(HMPA)_6]I_2$ was performed on a Hewlett-Packard 8452A diode array spectrophotometer. The UV−vis spectrum for $[Sm\{N(SiMe_3)_2\}_2]$ was determined on a SX.18 MV stopped-flow spectrophotometer (Applied Photophysics Ltd., Surrey, UK).

Stopped-Flow Rate Studies. Kinetic experiments in THF were performed with a computer controlled SX.18 MV stopped-flow spectrophotometer (Applied Photophysics Ltd., Surrey, UK). The $[Sm\{N(SiMe_3)_2\}_2]$ complex and substrates were taken separately in airtight Hamilton syringes from a drybox and injected into the stopped-flow system. The cellblock and the drive syringes of the stopped-flow reaction analyzer were flushed a minimum of three times with dry, degassed THF to make the system anaerobic. The concentration of $[Sm\{N(SiMe_3)_2\}_2]$ used for the study was 5 mM. The concentration of the substrates was kept high relative to $[Sm\{N(SiMe_3)_2\}_2]$ (0.05−0.45 M) to maintain pseudo first-order conditions. The pseudo first-order rate constants were determined using standard methods.[22] Reaction rates were determined from the decay of the $[Sm\{N(SiMe_3)_2\}_2]$ absorbance at 558 nm. The decay of the $Sm[N(SiMe_3)_2]_2$ complex displayed first-order behavior over >4 half-lives for all $[Sm\{N(SiMe_3)_2\}_2]$−substrate combinations. The kinetics for the ketones followed the rate law (1) shown below.

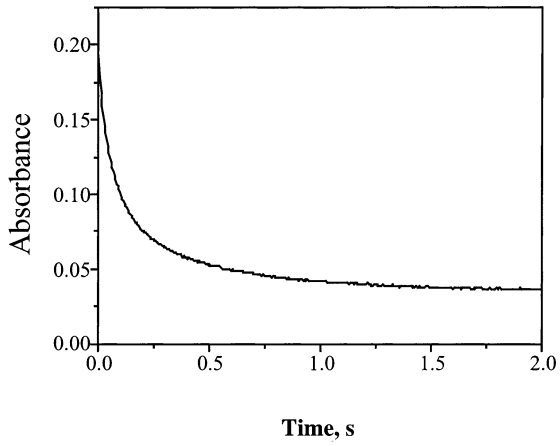

Figure 1. Stopped-flow trace showing the decay of $[Sm\{N(SiMe_3)_2\}_2]$ absorbance at 558 nm in the presence of 1-iodobutane (0.15 M) at 25 °C.

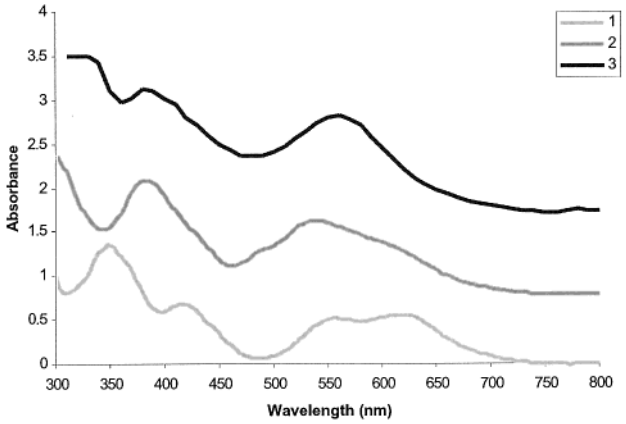

Figure 2. UV−vis spectra (stacked plot) for (1) SmI_2, (2) $[Sm(HMPA)_6]I_2$, and (3) $[Sm\{N(SiMe_3)_2\}_2]$.

$$-\text{d[Sm(II) complex]}/\text{d}t = k\text{[Sm(II) complex][ketone]} \quad (1)$$

The kinetics for the alkyl iodides followed the rate law (2) shown below.

$$-\text{d[Sm(II) complex]}/\text{d}t = 2k\text{[Sm(II) complex][alkyl iodide]} \quad (2)$$

A representative stopped-flow trace for the reduction of 1-iodobutane by $[Sm\{N(SiMe_3)_2\}_2]$ is contained in Figure 1. The temperature studies used to determine activation parameters were carried out over a range from 30 to 50 °C using a Neslab circulator connected to the sample handling unit of the stopped-flow system. The step size used for the temperature study was 5 °C, and each kinetic trace was recorded at a known temperature that was monitored by a thermocouple in the reaction cell. The temperature measurements are accurate to 0.01°.

Results

UV−Vis Spectroscopy. Figure 2 contains the UV−vis spectra of SmI_2, $[Sm(HMPA)_6]I_2$, and $[Sm\{N(SiMe_3)_2\}_2]$. The synthesis of $[Sm\{N(SiMe_3)_2\}_2]$ is carried out by adding 2 equiv of $NaN(SiMe_3)_2$ to SmI_2 in THF solvent. Addition of less than 2 equiv of $NaN(SiMe_3)_2$ produced a UV−vis spectrum consistent with SmI_2 and $[Sm\{N(SiMe_3)_2\}_2]$ exclusively. There are four primary absorbance regions for SmI_2 at 350, 416, 556, and 618 nm. The addition of 10 equiv of HMPA to SmI_2 forms $[Sm(HMPA)_6]I_2$. This complex has two broad prominent bands at 382 and 538 nm. The $[Sm\{N(SiMe_3)_2\}_2]$ complex has two prominent absorbances at 380 and 558 nm.

Cyclic Voltammetry. Cyclic voltammetry (CV) was utilized to estimate the thermodynamic redox potential of [Sm{N(Si-

(19) Evans, W. J.; Drummond, D. K.; Zhang, H.; Atwood, J. L. *Inorg. Chem.* **1988**, *27*, 575.
(20) Brady, E. D.; Clark, D. L.; Keogh, D. W.; Scott, B. L.; Watkin, J. G. *J. Am. Chem. Soc.* **2000**, *122*, 7007.
(21) Curran, D. P.; Gu, X.; Zhang, W.; Dowd, P. *Tetrahedron* **1997**, *53*, 9023.
(22) Pedersen, S. U.; Lund, T.; Daasbjerg, K.; Pop, M.; Fussing, I.; Lund, H. *Acta Chem. Scand.* **1998**, *52*, 657.

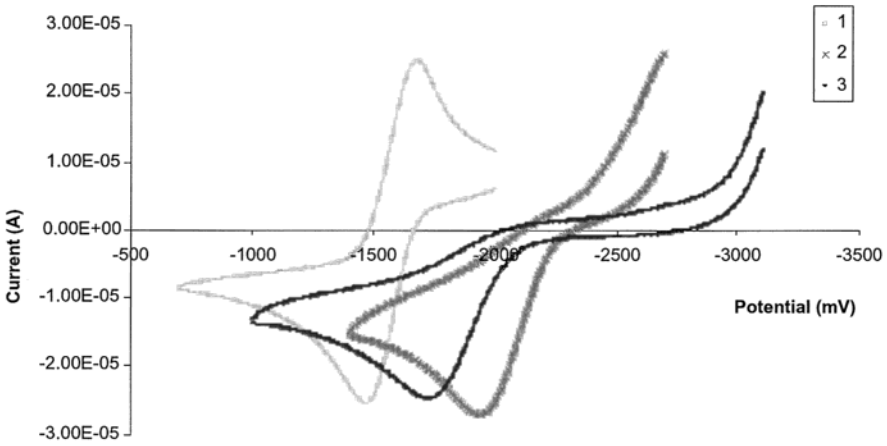

Figure 3. Cyclic voltammograms for (1) SmI_2, (2) $[Sm(HMPA)_6]I_2$, and (3) $[Sm\{N(SiMe_3)_2\}_2]$.

Table 1. Rate Constants and Activation Parameters for the Reduction of 1-Iodobutane by SmI_2, $[Sm(HMPA)_6]I_2$, and $[Sm\{N(SiMe_3)_2\}_2]$

system	k, (M^{-1} s^{-1})[b,c]	E_a, kcal mol^{-1} [d]	$\Delta S^{\ddagger}$, cal mol^{-1} K^{-1} [e]	$\Delta H^{\ddagger}$, kcal mol^{-1} [e]	$\Delta G^{\ddagger}$, kcal mol^{-1} [f]
SmI_2−1-iodobutane[a]	$(8 \pm 2) \times 10^{-4}$				
$[Sm(HMPA)_6]I_2$−1-iodobutane[a]	2.6 ± 0.1	9.3 ± 0.2	-28 ± 1	8.7 ± 0.2	17.3 ± 0.3
$[Sm\{N(SiMe_3)_2\}_2]$−1-iodobutane	19 ± 1	2.3 ± 0.1	-47 ± 1	1.7 ± 0.1	16.5 ± 0.3

[a] Initially reported in ref 24. [b] All rate data are the average of at least two independent runs. [c] Experimental uncertainties were propagated through these calculations, and all values are reported as $\pm\sigma$. [d] Calculated from $E_a = \Delta H^{\ddagger} + RT$. [e] Eyring activation parameters were obtained from $\ln(k_{obs}h/kT) = -\Delta H^{\ddagger}/RT + \Delta S^{\ddagger}/R$. [f] Calculated from $\Delta G^{\ddagger} = \Delta H^{\ddagger} - T\Delta S^{\ddagger}$.

Me$_3$)$_2$}$_2$] allowing comparison of potentials to those known for SmI_2 and $[Sm(HMPA)_6]I_2$.[12d,e,23] Figure 3 shows the CV data for SmI_2, $[Sm(HMPA)_6]I_2$, and $[Sm\{N(SiMe_3)_2\}_2]$. The potentials (vs $Ag/AgNO_3$) are -1.58 ± 0.04, -2.35 ± 0.03, and -2.1 ± 0.1, respectively.

Stopped-Flow Rate Studies. The rate constant for reduction of 1-iodobutane by $[Sm\{N(SiMe_3)_2\}_2]$ was determined in THF. The data along with results from 1-iodobutane reduction by SmI_2 and $[Sm(HMPA)_6]I_2$ determined previously are displayed in Table 1. While the rate of reduction of 1-iodobutane by SmI_2 is a slow process,[24] the addition of HMPA greatly enhances the reaction rate. Surprisingly, reduction of 1-iodobutane by $[Sm\{N(SiMe_3)_2\}_2]$ is faster than $[Sm(HMPA)_6]I_2$ by nearly an order of magnitude.

Reaction rates were determined over a range 30−50 °C to obtain activation parameters from the linear form of the Eyring equation (3). Figure 4 contains the Eyring plot for the reduction of 1-iodobutane by

$$\ln(k_{obs}h/kT) = -\Delta H^{\ddagger}/RT + \Delta S^{\ddagger}/R \qquad (3)$$

$[Sm\{N(SiMe_3)_2\}_2]$. Comparison of the activation parameters in Table 1 reveals some interesting differences between $[Sm\{N(SiMe_3)_2\}_2]$ and $[Sm(HMPA)_6]I_2$. While the rate constants for reduction are within an order of magnitude of each other and this difference is reflected by a modest change in the $\Delta G^{\ddagger}$ values (16.5 kcal/mol for $Sm[N(SiMe_3)_2]_2$ and 17.3 kcal/mol for $[Sm(HMPA)_6]I_2$), the major variance between the two complexes is shown by the enthalpic and entropic components of the activated complexes. The reduction of 1-iodobutane by $Sm[N(SiMe_3)_2]_2$ has a low barrier for $\Delta H^{\ddagger}$ and E_a (1.7 and 2.3 kcal/mol, respectively) as compared to reduction by $[Sm(HMPA)_6]I_2$ (8.7 and 9.3 kcal/mol, respectively). The entropy of activation for reduction by $[Sm\{N(SiMe_3)_2\}_2]$ is 19 eu's more negative than that for iodide reduction by $[Sm(HMPA)_6]I_2$.

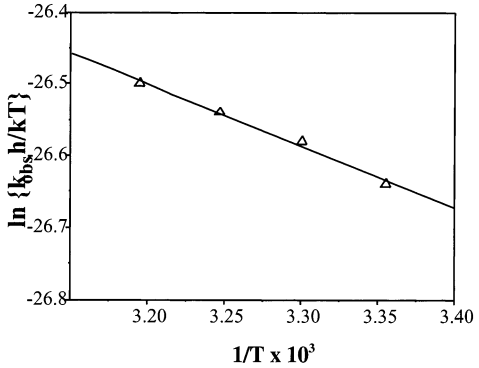

Figure 4. Erying plot for the $[Sm\{N(SiMe_3)_2\}_2]$/1-iodobutane system.

Next the kinetics of reduction of 2-butanone and methylacetoactetate by $[Sm\{N(SiMe_3)_2\}_2]$ were examined. The data along with rate data for reduction of the same substrates by SmI_2 and $[Sm(HMPA)_6]I_2$ are contained in Table 2. In the case of 2-butanone, reduction by SmI_2 is a slow process and within the same order of magnitude as the natural decay of SmI_2 in THF.[25] The addition of HMPA to SmI_2 increases the rate of reduction by an order of magnitude. Surprisingly, reduction of 2-butanone by $[Sm\{N(SiMe_3)_2\}_2]$ is significantly faster than reduction by $[Sm(HMPA)_6]I_2$. Comparison of the activation data for the reduction of 2-butanone by $[Sm(HMPA)_6]$ and $[Sm\{N(SiMe_3)_2\}_2]$ yielded interesting results. The $\Delta S^{\ddagger}$ values for reduction by both complexes are the same (within experimental error), while the barrier for reduction is substantially lower for the $[Sm\{N(SiMe_3)_2\}_2]$−2-butanone system. Rate constants for reduction of methylacetoacetate by SmI_2, $[Sm(HMPA)_6]I_2$, and $[Sm\{N(SiMe_3)_2\}_2]$ are 0.2, 9, and 2×10^3 M^{-1} s^{-1}, respectively.

(23) (a) Shabangi, M.; Kuhlman, M. L.; Flowers, R. A., II. *Org. Lett.* **1999**, *1*, 2133. (b) Enemaerke, R. J.; Daasbjerg, K.; Skrydstrup, T. *Chem. Commun.* **1999**, 343.
(24) Prasad, E.; Flowers, R. A., II. *J. Am. Chem. Soc.* **2002**, *124*, 6895.
(25) Prasad, E.; Flowers, R. A., II. *J. Am. Chem. Soc.* **2002**, *124*, 6357.

Table 2. Rate Constants and Activation Parameters for the Reduction of 2-Butanone and Methylacetoacetate by SmI_2, $[Sm(HMPA)_6]I_2$, and $[Sm\{N(SiMe_3)_2\}_2]$

system	k, $(M^{-1}\,s^{-1})^{b,c}$	E_a, kcal mol^{-1} [d]	$\Delta S^{\ddagger}$, cal mol^{-1} K^{-1} [e]	$\Delta H^{\ddagger}$, kcal mol^{-1} [e]	$\Delta G^{\ddagger}$, kcal mol^{-1} [f]
SmI_2−2-butanone[a]	$(7 \pm 3) \times 10^{-4}$				
$[Sm(HMPA)_6]I_2$−2-butanone[a]	$(8 \pm 1) \times 10^{-3}$	7.3 ± 0.3	-44 ± 1	6.7 ± 0.3	20.3 ± 0.4
$[Sm\{N(SiMe_3)_2\}_2]$−2-butanone	$(1.7 \pm 0.3) \times 10^{2}$	2.0 ± 0.3	-43 ± 1	1.4 ± 0.3	14.8 ± 0.6
SmI_2−methylacetoacetate[a]	$(2.0 \pm 0.4) \times 10^{-1}$	17 ± 1	-6 ± 1	16 ± 1	18 ± 1
$[Sm(HMPA)_6]I_2$−methylacetoacetate[a]	9 ± 2	3.5 ± 0.2	-43 ± 1	2.8 ± 0.2	16.3 ± 0.5
$[Sm\{N(SiMe_3)_2\}_2]$−methylacetoacetate[g]	$(2.0 \pm 0.2) \times 10^{3}$	nd	nd	nd	nd

[a] Initially reported in ref 24. [b] All rate data are the average of at least two independent runs. [c] Experimental uncertainties were propagated through these calculations, and all values are reported as $\pm\sigma$. [d] Calculated from $E_a = \Delta H^{\ddagger} + RT$. [e] Eyring activation parameters were obtained from $\ln(k_{obs}h/kT) = -\Delta H^{\ddagger}/RT + \Delta S^{\ddagger}/R$. [f] Calculated from $\Delta G^{\ddagger} = \Delta H^{\ddagger} - T\Delta S^{\ddagger}$. [g] The rate constant was found to be insensitive to changes in temperature; nd: not determined.

Attempts to determine activation parameters for the reduction of methylacetoacetate by $[Sm\{N(SiMe_3)_2\}_2]$ were unsuccessful because the rate of the reaction was temperature independent.

Discussion

Inspection of the crystal structure of $[Sm\{N(SiMe_3)_2\}_2]$ reveals some interesting features and differences from those published for $[SmI_2(THF)_5]$,[26] $[SmI_2HMPA_4]$,[12a] and $[Sm(HMPA)_6]I_2$.[12b] In particular, the two nitrogen donor atoms from the hexamethyldisilazide ligands and the two oxygen donor atoms (from THF) form a pseudo tetrahedral geometry around the samarium atom. Furthermore, one methyl on each of the silicon atoms is oriented toward the samarium atom as well, and each of the Sm−C bond distances for the distorted methyl group is smaller than the sum of their van der Waals radii.[19] The bent structure of this molecule is more reminiscent of $Sm(C_5Me_5)_2$ than SmI_2 and its associated HMPA complexes. The uncharacteristic bent shape of $[Sm\{N(SiMe_3)_2\}_2]$ should provide an increased probability for interaction between the metal center and organic substrates, assuming THF is easily displaced during the course of the reaction. This analysis suggests that $[Sm\{N(SiMe_3)_2\}_2]$ should be more reactive than SmI_2 and SmI_2−HMPA complexes. The goal of this work was to study the reactivity of $[Sm\{N(SiMe_3)_2\}_2]$ and compare it to SmI_2 and SmI_2−HMPA reductants to test the hypothesis described above.

Spectroscopy provides a convenient and straightforward method for studying Sm(II) reductants. The results in Figure 2 clearly show that each of the Sm(II) reductants described above has a unique UV−vis spectrum. The original report of Evans on the THF solvate of $[Sm\{N(SiMe_3)_2\}_2]$ also describes the structure and synthesis of $\{[(Me_3Si)_2N]Sm(\mu\text{-}I)(DME)(THF)_2\}$.[19] The synthesis of this complex was carried out by the combination of an equivalent amount of $SmI_2(THF)_2$ and $[Sm\{N(SiMe_3)_2\}_2]$ in THF/DME. During the preparation of $[Sm\{N(SiMe_3)_2\}_2]$, we monitored the UV−vis spectrum as increasing amounts of $NaN(SiMe_3)_2$ were added to SmI_2 in THF to ensure complete formation of the desired complex. The addition of less than 2 equiv of $NaN(SiMe_3)_2$ produced spectra consistent with SmI_2 and $[Sm\{N(SiMe_3)_2\}_2]$, exclusively. No evidence was observed in THF for the mixed Sm(II) species.[27] Further studies were carried out by examining UV−vis spectra over a series of concentrations from 0.005 to 0.02 M. No changes in the spectra were observed, indicating that $[Sm\{N(SiMe_3)_2\}_2]$ is stable in the concentration range utilized in the electrochemical and rate studies.

The bands between 500 and 650 nm for Sm(II) complexes have been attributed to f−d transitions.[28] McClure[29] and Johnson[30] have proposed energy level diagrams for f−d transitions to provide a satisfactory explanation for absorption of Ln(II) elements. A 1984 review by Kamenskaya cautions that the complexity and large number of energy states of the f−d transition make assignment of these bands difficult.[31] Regardless of the identity of the bands, these spectra clearly show that changing the coordination sphere around the Sm nucleus alters the ground- and excited-state orbitals, making each a unique reductant. The CV data also show that each Sm reductant is unique in terms of its thermodynamic redox potential, with $[Sm\{N(SiMe_3)_2\}_2]$ being intermediate (in terms of reducing power) between SmI_2 and $[Sm(HMPA)_6]I_2$.

Examination of the rate and activation parameters for the reduction of 1-iodobutane yields interesting results. Reduction of the alkyl iodide by $[Sm\{N(SiMe_3)_2\}_2]$ is faster than reduction by $[Sm(HMPA)_6]I_2$ even though the former is a less powerful reductant (based on redox potentials). Recent rate and mechanistic studies from our lab indicate that the electron transfer (ET) from Sm−(HMPA) complexes to alkyl iodides has an outer-sphere component.[24] If the reduction of 1-iodobutane by $[Sm\{N(SiMe_3)_2\}_2]$ occurred through an outer-sphere process, the rate would be expected to correlate with the redox potential of the reductant. Examination of the rate data in Table 1 shows this is clearly not the case. Because the activation parameters obtained from the kinetic studies of the three Sm complexes include contributions from solvent, care must be taken in their interpretation and comparison with one another. Nonetheless, in qualitative terms, the large negative $\Delta S^{\ddagger}$ and small $\Delta H^{\ddagger}$ for reduction of 1-iodobutane by $[Sm\{N(SiMe_3)_2\}_2]$ are consistent with an ordered transition state containing a high degree of interaction between the metal center and substrate (Scheme 1). All of these results taken together suggest that the mechanism of reduction of the alkyl iodide by $[Sm\{N(SiMe_3)_2\}_2]$ has more inner-sphere character than reduction by SmI_2 or Sm−(HMPA) complexes.

Inspection of the kinetic results obtained for the reduction of 2-butanone and methylacetoacetate shows even more dramatic results than those obtained for 1-iodobutane. In the case of 2-butanone, the rate of reduction by $[Sm\{N(SiMe_3)_2\}_2]$ is 4 orders of magnitude faster than reduction by $[Sm(HMPA)_6]I_2$.

(26) Evans, W. J.; Gummersheimer, T. S.; Ziller, J. W. *J. Am. Chem. Soc.* **1995**, *117*, 8999.
(27) In the original preparation of this compound, Evans and co-workers found that formation of the mixed Sm complex was reversible under appropriate conditions. When a solution of $\{[(Me_3Si)_2N]Sm(\mu\text{-}I)(DME)(THF)_2\}$ was cooled, $SmI_2(THF)_2$ precipitated leaving a solution of $\{Sm[N(SiMe_3)_2]_2(thf)_2\}$. Details are contained in ref 19.
(28) Okaue, Y.; Isobe, T. *Inorg. Chem. Acta* **1988**, *144*, 143.
(29) McClure, D. S.; Kiss, Z. *J. Chem. Phys.* **1963**, *39*, 3251.
(30) Johnson, K. E.; Sandoe, J. N. *J. Chem. Soc. A* **1960**, 1694.
(31) Kamenskaya, A. N. *Russ. J. Inorg. Chem.* **1984**, *29*, 251.

Scheme 1

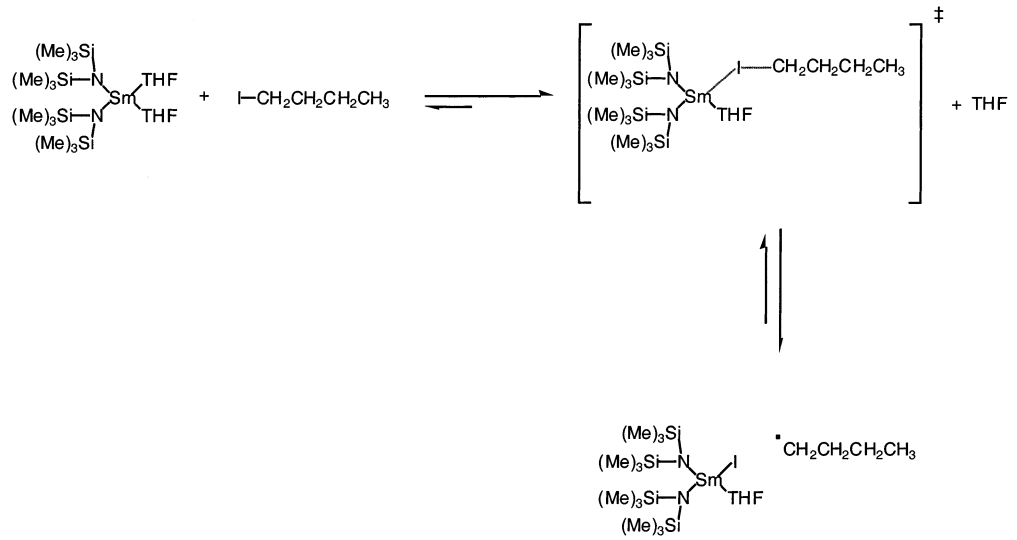

The low barrier for $\Delta H^{\ddagger}$ and E_a (1.4 and 2.0 kcal/mol, respectively) and the negative $\Delta S^{\ddagger}$ of −43 eu's is consistent with a strong interaction between [Sm{N(SiMe$_3$)$_2$}$_2$] and 2-butanone in the activated complex. Reduction of methylacetoacetate by [Sm{N(SiMe$_3$)$_2$}$_2$] is faster than reduction of 2-butanone by 2 orders of magnitude, a result consistent with chelation between the reductant and substrate.[25] The rate of reduction of methylacetoacetate by [Sm{N(SiMe$_3$)$_2$}$_2$] was found to be insensitive to changes in temperature over the range examined, and, as a result, the enthalpy of activation could not be determined for this system. The insensitivity of the rate constant to temperature change is one indication of an inner-sphere ET.[32]

Comparison of the rates of reduction of 1-iodobutane and the ketones also provides some insight into the potential synthetic use and pitfalls of using [Sm{N(SiMe$_3$)$_2$}$_2$] instead of SmI_2 or SmI_2−HMPA in organic synthesis. Recent work from our group clearly shows that both primary and secondary alkyl iodides are reduced faster by SmI_2−HMPA complexes than are dialkyl ketones.[24] The selective reduction of alkyl iodides by SmI_2−HMPA to produce an organosamarium intermediate which then attacks a ketone is the determining factor in the success of the samarium Barbier reaction.[33] Conversely, the data above clearly indicate that [Sm{N(SiMe$_3$)$_2$}$_2$] reduces 2-butanone faster than 1-iodobutane. This finding implies that the Sm-silylamide complex will be unsuitable for reductive coupling of alkyl halides and ketones run under Barbier conditions, but may be appropriate for halide-carbonyl coupling reactions run under Grignard-type conditions. The affinity of [Sm{N(SiMe$_3$)$_2$}$_2$] for ketones should make it useful in the reductive coupling of carbonyls with olefins and other radical-based reactions where cyclization or addition occurs faster than radical reduction.

(32) Hubig, S. M.; Rathore, R.; Kochi, J. K. *J. Am. Chem. Soc.* **1999**, *121*, 617.
(33) (a) Curran, D. P.; Totleben, M. J. *J. Am. Chem. Soc.* **1992**, *114*, 6050. (b) Curran, D. P.; Fevig, T. L.; Jasperse, C. P.; Totleben, M. J. *Synlett* **1992**, 943.

Conclusions

Changing the ligands on Sm(II) reductants can have a profound impact on reactivity. Although the redox potential (reducing power) of [Sm{N(SiMe$_3$)$_2$}$_2$] is intermediate between SmI_2 and [Sm(HMPA)$_6$]I$_2$, it reacts much faster with alkyl iodides and ketones. The rate and activation data presented herein are consistent with a change in the ET toward a larger inner-sphere component as compared to SmI_2 and SmI_2−HMPA. The change in ET mechanism can be attributed to the unique structure of the [Sm{N(SiMe$_3$)$_2$}$_2$] complex. From a practical point of view, replacement of HMPA with another ligand is advantageous because of its carcinogenicity, but, aside from this, the presence of the silylamide ligand also increases solubility of the Sm-based reductant in solvents other than THF. We are currently carrying out kinetic studies in a series of solvents to determine the role of solvation in Sm-mediated reactions. Synthetic studies are also being carried out to compare the synthetic utility of [Sm{N(SiMe$_3$)$_2$}$_2$] with SmI_2 and SmI_2−HMPA. This work will be reported in due course.

Acknowledgment. R.A.F. is grateful to the National Science Foundation (CHE-0196163) for support of this work. Acknowledgment is also made to the Robert A. Welch Foundation and the Petroleum Research Fund (35762-AC1) for partial support of this research. We thank Drs. Rebecca Miller and Leanne Miller for their useful comments on the manuscript.

Supporting Information Available: Decay traces and plots of rate data (PDF). This material is available free of charge via the Internet at http://pubs.acs.org.

JA028111G